

Structure Learning with Bow-free Acyclic Path Diagrams

Christopher Nowzohour*
Seminar für Statistik, ETH Zürich
nowzohour@stat.math.ethz.ch

Marloes H. Maathuis
Seminar für Statistik, ETH Zürich
maathuis@stat.math.ethz.ch

Peter Bühlmann
Seminar für Statistik, ETH Zürich
buhlmann@stat.math.ethz.ch

October 10, 2022

Abstract

We consider the problem of structure learning for bow-free acyclic path diagrams (BAPs). BAPs can be viewed as a generalization of linear Gaussian DAG models that allow for certain hidden variables. We present a first method for this problem using a greedy score-based search algorithm. We also investigate some distributional equivalence properties of BAPs which are used in an algorithmic approach to compute (nearly) equivalent model structures, allowing to infer lower bounds of causal effects. The application of our method to some datasets reveals that BAP models can represent the data much better than DAG models in these cases.

1 Introduction

We consider learning the causal structure among a set of variables from observational data. In general, the data can be modelled with a structural equation model (SEM) over the observed and unobserved variables, which expresses each variable as a function of its direct causes and a noise term, where the noise terms are assumed to be mutually independent. The structure of the SEM is visualized as a directed graph, with vertices representing variables and edges representing direct causal relationships. We assume

*Corresponding Author

the structure to be recursive (acyclic), which results in a directed acyclic graph (DAG). DAGs can be understood as models of conditional independence, and many structure learning algorithms use this to find all DAGs which are compatible with the observed conditional independencies (Spirtes et al., 1993). Often, however, not all relevant variables are observed. The resulting marginal distribution over the observed variables might still satisfy some conditional independencies, but in general these will not have a DAG representation (Richardson and Spirtes, 2002). Also, there generally are additional constraints resulting from the marginalization of some of the variables (Evans, 2014; Shpitser et al., 2014).

In this paper we consider a model class which can accommodate certain hidden variables. Specifically, we assume that the graph over the observed variables is a bow-free acyclic path diagram (BAP). This means it can have directed as well as bidirected edges (with the directed part being acyclic), where the directed edges represent direct causal effects, and the bidirected edges represent hidden confounders. The bow-freeness condition means there cannot be both a directed and a bidirected edge between the same pair of variables. The BAP can be obtained from the underlying DAG over all (hidden and observed) variables via a latent projection operation (Pearl, 2000) (if the bow-freeness condition admits this). We furthermore assume a parametrization with linear structural equations and Gaussian noise, where two noise terms are correlated only if there is a bidirected edge between the two respective nodes. For many practical purposes, it is beneficial to consider this restricted class of hidden variable models. Such a restricted model class, if not heavily misspecified, results in a smaller distributional equivalence class, and estimation is expected to be more accurate than for more general hidden variable methods like FCI (Spirtes et al., 1993), RFCI (Colombo et al., 2012), or FCI+ (Claassen et al., 2013).

The goal of this paper is structure learning with BAPs, that is, finding the best set of BAPs given some observational data. Just like in other models, there is typically an equivalence class of BAPs that are statistically indistinguishable, so a meaningful structure search result should represent this equivalence class. We propose a penalized likelihood score that is greedily optimized and a heuristic algorithm (supported by some theoretical results) for finding equivalent models once an optimum is found. This method is the first of its kind for BAP models.

Example of a BAP

Consider the situation shown in Figure 1a, where we observe variables X_1, \dots, X_4 , but do not observe H_1 . The only (conditional) independency over the observed variables is $X_1 \perp\!\!\!\perp X_3 \mid X_2$, which is also represented in the corresponding BAP in Figure 1b. The parametrization of this BAP would

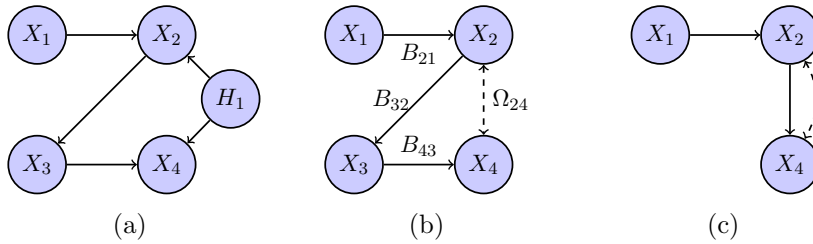


Figure 1: (a) DAG with hidden variable H_1 , (b) resulting BAP over the observed variables X_1, \dots, X_4 with annotated edge weights, and (c) resulting graph if X_3 is also not observed, which is not a BAP.

be

$$\begin{aligned}
 X_1 &= \epsilon_1 \\
 X_2 &= B_{21}X_1 + \epsilon_2 \\
 X_3 &= B_{32}X_2 + \epsilon_3 \\
 X_4 &= B_{43}X_3 + \epsilon_4
 \end{aligned}$$

with $(\epsilon_1, \epsilon_2, \epsilon_3, \epsilon_4)^T \sim \mathcal{N}(\mathbf{0}, \Omega)$ and

$$\Omega = \begin{pmatrix} \Omega_{11} & 0 & 0 & 0 \\ 0 & \Omega_{22} & 0 & \Omega_{24} \\ 0 & 0 & \Omega_{33} & 0 \\ 0 & \Omega_{24} & 0 & \Omega_{44} \end{pmatrix}.$$

Hence the model parameters in this case are $B_{21}, B_{32}, B_{43}, \Omega_{11}, \Omega_{22}, \Omega_{33}, \Omega_{44}$, and Ω_{24} . An example of a graph that is not a BAP is shown in Figure 1c.

Challenges

The main challenge, like with all structure search problems in graphical modelling, is the vastness of the model space. The number of BAPs grows super-exponentially. Exhaustively scoring all BAPs and finding the global score optimum is typically computationally infeasible.

Another major challenge, specifically for our setting, is the fact that a graphical characterization of the (distributional) equivalence classes for BAP models is not yet known. In the (unconstrained) DAG case, for example, it is known that models are equivalent if and only if they share the same skeleton and v-structures (Verma and Pearl, 1991). A similar result is not known for BAPs (or the more general acyclic directed mixed graphs). This makes it hard to traverse the search space efficiently, since one cannot search over the equivalence classes (like the greedy equivalence search for DAGs (Chickering, 2002)). It also makes it difficult to evaluate simulation results, since the ground truth BAP and the found solution might not coincide yet be equivalent.

Contributions

We provide the first structure learning algorithm for BAPs. It is a score-based algorithm and uses greedy hill climbing to optimize a penalized likelihood score. By decomposing the score over the bidirected connected components of the graph and caching the score of each component we are able to achieve a significant computational speedup. To mitigate the problem of local optima, we perform many random restarts of the greedy search.

We propose to approximate the distributional equivalence class of a BAP by using a greedy strategy for likelihood scoring. If two BAPs are similar with respect to their likelihoods within a tolerance, they should be treated as statistically indistinguishable and hence as belonging to the same class of (nearly) equivalent BAPs. Based on such greedily computed (near) equivalence classes, we can then infer bounds of total causal effects, in the spirit of Maathuis et al. (2009, 2010).

We present some theoretical results towards equivalence properties in BAP models, some of which generalize to acyclic path diagrams. We also provide a proof of Wright’s path tracing formula that does not assume a proper model parametrization. Furthermore, we developed a Markov Chain Monte Carlo method for uniformly sampling BAPs based on ideas from Kuipers and Moffa (2015).

We obtain promising results on simulated data sets despite the challenges listed above. Comparing the maximal penalized likelihood scores between BAPs and DAGs on real datasets shows a clear advantage of BAP models.

Related Work

There are two main research communities that intersect at this topic. On the one side there are the path diagram models, going back to Wright (1934) and then being mainly developed in the behavioral sciences (Jöreskog, 1970; Duncan, 1975; Glymour and Scheines, 1986; Jöreskog, 2001). In this setting there is always a parametric model, usually assuming linear edge functions and Gaussian noise. In the most general formulation, the graph over the observed variables is assumed to be an acyclic directed mixed graph (ADMG), which can have bows. While in general the parameters for these models are not identified, Drton et al. (2011) give necessary and sufficient conditions for global identifiability. Complete necessary and sufficient conditions for the more useful almost everywhere identifiability remain unknown. BAP models are a useful subclass, since they are almost everywhere identified (Brito and Pearl, 2002). Drton et al. (2009) provided an algorithm, called residual iterative conditional fitting (RICF), for maximum likelihood estimation of the parameters for a given BAP.

On the other side there are the non-parametric hidden variable models, which are defined as marginalized DAG models (Pearl, 2000). The marginal-

ized distributions are constrained by conditional independencies, as well as additional equality and inequality constraints (Evans, 2014). When just modelling the conditional independence constraints, the class of maximal ancestral graphs (MAGs) is sufficient (Richardson and Spirtes, 2002). Shpitser et al. (2014) have proposed the nested Markov model using ADMGs to also include the additional equality constraints. Finally, mDAGs can be used to model all resulting constraints (Evans, 2014). With each additional layer of constraints, learning the structure from data becomes more complicated, but at the same time more available information is utilized and a possibly more detailed structure can be learned. Ancestral BAP models coincide with the Gaussian parametrization of MAGs (Richardson and Spirtes, 2002, Section 8). However, in general BAPs need to be neither maximal nor ancestral and can model additional constraints. They are easier to interpret as hidden variable models. This can be seen when comparing the BAP in Figure 1b with the corresponding MAG. The latter would have an additional edge between X_1 and X_4 since there is no (conditional) independence of these two variables. As can be verified, the BAP and the MAG in this example are not distributionally equivalent, since the former encodes additional non-independence constraints.

Structure search for MAGs can be done with the FCI (Spirtes et al., 1993), RFCI (Maathuis et al., 2009), or FCI+ (Claassen et al., 2013) algorithms. Silva and Ghahramani (2006) propose a fully Bayesian method for structure search in linear Gaussian ADMGs, sampling from the posterior distribution using an MCMC approach. Shpitser et al. (2012) employ a greedy approach to optimize a penalized likelihood over ADMGs for discrete parametrizations.

Outline of this Paper

This paper is structured as follows. In Section 2 we give an in-depth overview of the model and its estimation from data, as well as some distributional equivalence properties. In Section 3 we present the details of our greedy algorithm with various computational speedups. In Section 4 we present empirical results on simulated and real datasets. All proofs as well as further theoretical results and justifications can be found in the Appendix.

2 Model and Estimation

2.1 Graph Terminology

Let X_1, \dots, X_d be a set of random variables and $V = \{1, \dots, d\}$ be their index set. The elements of V are also called *nodes* or *vertices*. A *mixed graph* or *path diagram* G on V is an ordered tuple $G = (V, E_D, E_B)$ for some $E_D, E_B \subset V \times V$. If $(i, j) \in E_D$, we say there is a *directed edge* from i to

j and write $i \rightarrow j \in G$. If $(i, j) \in E_B$, we must also have $(j, i) \in E_B$, and we say there is a *bidirected edge* between i and j and write $i \leftrightarrow j \in G$. The set $\text{pa}_G(i) := \{j \mid j \rightarrow i \in G\}$ is called the *parents* of i . This definition extends to sets of nodes S in the obvious way: $\text{pa}_G(S) := \bigcup_{i \in S} \text{pa}_G(i)$. The *in-degree* of i is the number of arrowheads at i . If $V' \subseteq V$, $E'_D \subseteq E_D|_{V' \times V'}$, and $E'_B \subseteq E_B|_{V' \times V'}$, then $G' = (V', E'_D, E'_B)$ is called a *subgraph* of G , and we write $G' \subseteq G$. If any of the subset relations are strict, we call G' a *strict subgraph* of G and write $G' \subset G$. The *skeleton* of G is the undirected graph over the same node set V and with edges $i - j$ if and only if $i \rightarrow j \in G$ or $i \leftrightarrow j \in G$ (or both).

A *path* π between i and j is an ordered tuple of (not necessarily distinct) nodes $\pi = (v_0 = i, \dots, v_l = j)$ such that there is an edge between v_k and v_{k+1} for all $k = 0, \dots, l-1$. If the nodes are distinct, the path is called *non-overlapping*. The *length* of π is the number of edges $\lambda(\pi) = l$. If π consists only of directed edges pointing in the direction of j , it is called a *directed path* from i to j . The tuple (i, j, k) is called a *collider* on π if i, j and j, k are each adjacent on π with arrowheads pointing from i to j and from k to j ¹. If additionally there is no edge between i and k (and $i \neq k$), the collider is called *v-structure*. A path without colliders is called a *trek*.

Let $A, B, C \subset V$ be three disjoint sets of nodes. The set $\text{an}(C) := C \cup \{i \in V \mid \text{there exists a directed non-overlapping path from } i \text{ to } c \text{ for some } c \in C\}$ is called the *ancestors* of C . A non-overlapping path π from $a \in A$ to $b \in B$ is said to be *m-connecting given C* if every non-collider on π is not in C and every collider on π is in $\text{an}(C)$. If there are no such paths, A and B are *m-separated given C*, and we write $A \perp\!\!\!\perp_m B \mid C$. We use a similar notation for denoting conditional independence of the corresponding set of variables X_A and X_B given X_C : $X_A \perp\!\!\!\perp X_B \mid X_C$.

A graph G is called *cyclic* if there are at least two nodes i and j such that there are directed paths both from i to j and from j to i . Otherwise G is called *acyclic* or *recursive*. An acyclic path diagram is also called an acyclic directed mixed graph (ADMG). An acyclic path diagram having at most one edge between each pair of nodes is called a *bow-free*² *acyclic path diagram (BAP)*. An ADMG without any bidirected edges is called a *directed acyclic graph (DAG)*.

2.2 The Model

A *linear structural equation model (SEM)* M is a set of linear equations involving the variables $\mathbf{X} = (X_1, \dots, X_d)^T$ and some error terms $\boldsymbol{\epsilon} = (\epsilon_1, \dots, \epsilon_d)^T$:

$$\mathbf{X} = B\mathbf{X} + \boldsymbol{\epsilon}, \quad (1)$$

¹That is, one of the following structures: $\rightarrow\leftarrow, \leftrightarrow\leftarrow, \rightarrow\leftrightarrow, \leftrightarrow\leftrightarrow$.

²The structure $i \rightarrow j$ together with $i \leftrightarrow j$ is also known as *bow*.

where B is a real matrix, and $\text{cov}(\epsilon) = \Omega$ is a positive semi-definite matrix. M has an associated graph G that reflects the structure of B and Ω . For every non-zero entry B_{ij} there is a directed edge from j to i , and for every non-zero entry Ω_{ij} there is a bidirected edge between i and j . Thus we can also write (1) as:

$$X_i = \sum_{j \in \text{pa}_G(i)} B_{ij} X_j + \epsilon_i, \quad \text{for all } i \in V, \quad (2)$$

with $\text{cov}(\epsilon_i, \epsilon_j) = \Omega_{ij}$ for all $i, j \in V$.

Our model is a special type of SEM; in particular, we make the following assumptions:

(A1) The errors ϵ follow a multivariate Normal distribution $\mathcal{N}(\mathbf{0}, \Omega)$.

(A2) The associated graph G is a BAP.

It then follows from (A1) that M is completely parametrized by $\theta = (B, \Omega)$. Often M is specified via its graph G , and we are interested to find a parametrization θ_G compatible with G . We thus define the parameter spaces for the edge weight matrices B (directed edges) and Ω (bidirected edges) for a given BAP G as

$$\begin{aligned} \mathcal{B}_G &= \{B \in \mathbb{R}^{d \times d} \mid B_{ij} = 0 \text{ if } j \rightarrow i \text{ is not an edge in } G\} \\ \mathcal{O}_G &= \{\Omega \in \mathbb{R}^{d \times d} \mid \Omega_{ij} = 0 \text{ if } i \neq j \text{ and } i \leftrightarrow j \text{ is not an edge in } G; \\ &\quad \Omega \text{ is positive semi-definite}\} \end{aligned}$$

and the combined parameter space as

$$\Theta_G = \mathcal{B}_G \times \mathcal{O}_G.$$

The covariance matrix for \mathbf{X} is given by:

$$\phi(\theta) = (I - B)^{-1} \Omega (I - B)^{-T}, \quad (3)$$

where $\phi : \Theta_G \rightarrow \mathcal{S}_G$ maps parameters to covariance matrices, and $\mathcal{S}_G := \phi(\Theta_G)$ is the set of covariance matrices compatible with G . Note that $\phi(\theta)$ exists since G is acyclic by (A2) and therefore $I - B$ is invertible.

We assume that the variables are normalized to have variance 1, that is, we are interested in the subset $\bar{\mathcal{S}}_G \subset \mathcal{S}_G$, where $\bar{\mathcal{S}}_G = \{\Sigma \in \mathcal{S}_G \mid \Sigma_{ii} = 1 \text{ for all } i = 1, \dots, d\}$, and its preimage under ϕ , $\bar{\Theta}_G := \phi^{-1}(\bar{\mathcal{S}}_G) \subset \Theta_G$.

One of the main motivations of working with BAP models is parameter identifiability. This is defined below:

Definition 1. *A normalized parametrization $\theta_G \in \bar{\Theta}_G$ is identifiable if there is no $\theta'_G \in \bar{\Theta}_G$ such that $\theta_G \neq \theta'_G$ and $\phi(\theta_G) = \phi(\theta'_G)$.*

Brito and Pearl (2002) show that for any BAP G , the set of normalized non-identifiable parametrizations has measure zero.

The causal interpretation of BAPs is the following. A directed edge from X to Y represents a direct causal³ effect of X on Y . A bidirected edge between X and Y represents a hidden variable which is a direct cause of both X and Y . In practice, one is often interested in predicting the effect of an intervention at X_i on another variable X_j . This is called the *total causal effect* of X_i on X_j and can be defined as $E_{ij} = \frac{\partial}{\partial x} \mathbb{E}[X_j \mid do(X_i = x)]$, where the $do(X_i = x)$ means replacing the respective equation in (2) with $X_i = x$ (Pearl, 2000). For linear Gaussian path diagrams this is a constant quantity and given by

$$E_{ij} = ((I - B)^{-1})_{ij}. \quad (4)$$

2.3 Penalized Maximum Likelihood

Consider a BAP G . A first objective is to estimate the parameters θ_G from i.i.d. samples $\{x_i^{(s)}\}$ ($i = 1, \dots, d$ and $s = 1, \dots, n$). This can be done by maximum likelihood estimation using the RICF method of Drton et al. (2009). Given the Gaussianity assumption (A1) and the covariance formula (3), one can write down the log-likelihood for a given parameter set θ_G and a sample covariance matrix S :

$$l(\theta_G; S) = -\frac{n}{2} \left(\log |2\pi\Sigma_G| + \frac{n-1}{n} \text{tr}(\Sigma_G^{-1}S) \right), \quad (5)$$

where $\Sigma_G = \phi(\theta_G)$ is the covariance matrix implied by parameters θ_G , see for example Mardia et al. (1979, (4.1.9)). However, due to the structural constraints on B and Ω it is not straightforward to maximize this for θ_G . RICF is an iterative method to do so, yielding the maximum likelihood estimate:

$$\hat{\theta}_G = \arg \max_{\theta_G \in \Theta_G} l(S; \theta_G). \quad (6)$$

We now extend this to the scenario where the graph G is also unknown, using a regularized likelihood score with a BIC-like penalty term that increases with the number of edges. Concretely, we use the following score for a given BAP G :

$$s(G) := \frac{1}{n} \left(\max_{\theta_G \in \Theta_G} l(S; \theta_G) - (\#\{\text{nodes}\} + \#\{\text{edges}\}) \log n \right). \quad (7)$$

We have scaled the log-likelihood and penalty with $1/n$ so that the score converges to a limit⁴ for increasing n . Compared with the usual BIC penalty,

³We adopt the *interventional* definition of causality, i.e. there is a direct causal effect of X on Y if intervening at X changes Y .

⁴For the true graph G , this limit is the negative entropy of the joint distribution.

we chose our penalty to be twice as large, since this led to better performance in simulations studies.

2.4 Equivalence Properties

There is an important issue when doing structure learning with graphical models: typically the maximizers of (7) will not be unique. This is a fundamental problem for most model classes and a consequence of the model being underdetermined. In general, there are sets of graphs that are statistically indistinguishable (in the sense that they can all parametrize the same joint distributions over the variables). These graphs are called *distributionally equivalent*. For nonparametric DAG models (without non-linearity or non-Gaussianity constraints), for example, the distributional equivalence classes are characterized by conditional independencies and are called Markov equivalence classes. For BAPs, distributional equivalence is not completely characterized yet, but we can present some useful results (see Spirtes et al. (1998) or Williams (2012) for a discussion of the linear Gaussian ADMG case). Let us first make precise the different notions of model equivalence.

Definition 2. *Two BAPs G_1, G_2 over a set of nodes V are Markov equivalent if they imply the same m -separation relationships.*

This essentially means they imply the same conditional independencies, and the definition coincides with the classical notion of Markov equivalence for DAGs. The following notion of distributional equivalence is stronger.

Definition 3. *Two BAPs G_1, G_2 are distributionally equivalent if for all $\theta_{G_1} \in \bar{\Theta}_{G_1}$ there exists $\theta_{G_2} \in \bar{\Theta}_{G_2}$ (and vice versa) such that $\phi(\theta_{G_1}) = \phi(\theta_{G_2})$.*

Spirtes et al. (1998) showed the following global Markov property for general linear path diagrams: if there are nodes $a, b \in V$ and a possibly empty set $C \subset V$ such that $a \perp\!\!\!\perp_m b \mid C$, then the partial correlation of X_a and X_b given X_C is zero. As a direct consequence, we get the following first result:

Theorem 1. *If two BAPs G_1, G_2 do not share the same m -separations, they are not distributionally equivalent.*

Unlike for DAGs, the converse is not true, as the counterexample in Figure 2 shows.

An important tool in this context is Wright’s path tracing formula (Wright, 1960), which expresses the covariance between any two variables in a path diagram as the sum-product over the edge labels of the treks (collider-free paths) between those variables, as long as all variables are normalized to

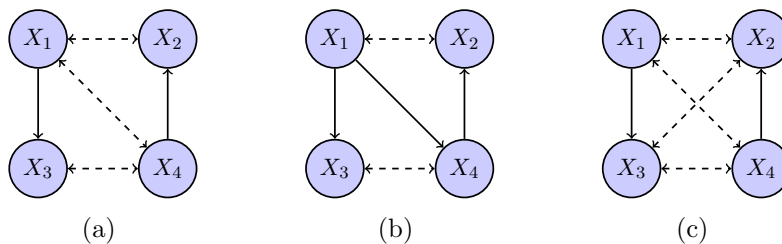


Figure 2: The two BAPs in (a) and (b) share the same skeleton and v-structures, but in (a) there are no m-separations, whereas in (b) we have $X_2 \perp\!\!\!\perp_m X_3 \mid \{X_1, X_4\}$. BAPs (a) and (c) share the same m-separations (none) but are not distributionally equivalent since (a) is a strict subgraph of (b) (using Theorem 3).

variance 1. A precise statement as well as a proof of a more general version of Wright’s formula can be found in the Appendix (Theorem 5). As an example, consider the BAP in Figure 1b. There are two treks between X_2 and X_4 : $X_2 \rightarrow X_3 \rightarrow X_4$ and $X_2 \leftrightarrow X_4$. Hence $\text{cov}(X_2, X_4) = B_{32}B_{43} + \Omega_{24}$, assuming normalized parameters. Similarly we have $\text{cov}(X_1, X_4) = B_{21}B_{32}B_{43}$.

As a consequence of Wright’s formula, we can show that having the same skeleton and collider structure is sufficient for two acyclic path diagrams to be distributionally equivalent (Theorem 2 below). For DAGs, it is known that the weaker condition of having the same skeleton and v-structures is sufficient for being Markov equivalent. However, for BAPs this is not true, as the counterexample in Figure 2 shows.

Theorem 2. *Let G_1, G_2 be two acyclic path diagrams that have the same skeleton and collider structure. Then G_1 and G_2 are distributionally equivalent.*

It would be desirable to also have a necessary condition for distributional equivalence. We conjecture that having the same skeleton is a necessary condition. For DAGs this is trivial, since a missing edge between two nodes means they can be d-separated, and thus a conditional independency would have to be present in the corresponding distribution. However, for BAPs a missing edge does not necessarily result in an m-separation, as the counterexample in Figure 2 shows. The following theorem at least shows that strictly nested models cannot be distributionally equivalent.

Theorem 3. *Let G_1, G_2 be two BAPs over the same set of nodes, such that G_1 is a strict subgraph of G_2 . Then G_1 and G_2 are not distributionally equivalent.*

3 Greedy Search

We aim to find the maximizer of (7) over all graphs over the node set $V = \{1, \dots, d\}$. Since exhaustive search is infeasible, we use greedy hill-climbing. Starting from some graph G^0 , this method obtains increasingly better estimates by exploring the local neighborhood of the current graph. At the end of each exploration, the highest-scoring graph is selected as the next estimate. This approach is also called greedy search and is often used for combinatorial optimization problems. Greedy search converges to a local optimum, although typically not the global one. To alleviate this we repeat it multiple times with different (random) starting points.

We use the following neighborhood relation. A BAP G' is in the *local neighborhood* of G if it differs by exactly one edge, that is, one of the following holds:

1. $G \subset G'$ (edge addition),
2. $G' \subset G$ (edge deletion), or
3. G and G' have the same skeleton (edge change).

If we only admit the first condition, the procedure is called *forward search*, and it is usually started with the empty graph. Instead of at every step searching through the complete local neighborhood (which can become prohibitive for large graphs), we can also select a random subset of neighbors and only consider those.

In Sections 3.1 and 3.2 we describe some adaptations of this general scheme, that are specific to the problem of BAP learning. In Section 3.3 we describe our greedy equivalence class algorithm.

3.1 Score Decomposition

Greedy search becomes much more efficient when the score separates over the nodes or parts of the nodes. For DAGs, for example, the log-likelihood can be written as a sum of components, each of which only depends on one node and its parents. Hence, when considering a neighbor of some given DAG, one only needs to update the components affected by the respective edge change. A similar property holds for BAPs. Here, however, the components are not the nodes themselves, but rather the connected components of the bidirected part of the graph (that is, the partition of V into sets of vertices that are reachable from each other by only traversing the bidirected edges). For example, in Figure 1b the bidirected connected components (sometimes also called districts) are $\{X_1\}$, $\{X_2, X_4\}$, $\{X_3\}$. This decomposition property is known (Richardson, 2009), but for completeness we give a derivation in the Appendix. We write out the special case of the Gaussian parametrization below.

Let us write $p_G^{\mathbf{X}}$ for the joint density of \mathbf{X} under the model (2), and p_G^ϵ for the corresponding joint density of ϵ . Let C_1, \dots, C_K be the connected components of the bidirected part of G . We separate the model G into submodels G_1, \dots, G_K of the full SEM (2), where each G_k consists only of nodes in $V_k = C_k \cup \text{pa}(C_k)$ and without any edges between nodes in $\text{pa}(C_k)$. Then, as we show in the Appendix, the log-likelihood of the model with joint density $p_G^{\mathbf{X}}$ given data $\mathcal{D} = \{x_i^{(s)}\}$ (with $1 \leq i \leq d$ and $1 \leq s \leq n$) can be written as:

$$\begin{aligned} l(p_G^{\mathbf{X}}; \mathcal{D}) &= \sum_{s=1}^n \log p_G^{\mathbf{X}}(x_1^{(s)}, \dots, x_p^{(s)}) \\ &= \sum_k \left(l(p_{G_k}^{\mathbf{X}}; \{x_i^{(s)}\}_{i \in V_k}^{s=1, \dots, n}) - \sum_{j \in \text{pa}(C_k)} l(p_{G_k}^{\mathbf{X}}; \{x_j^{(s)}\}_{s=1, \dots, n}) \right), \end{aligned}$$

where $l(p_{G_k}^{\mathbf{X}}; \{x_j^{(s)}\}_{s=1, \dots, n})$ refers to the likelihood of the X_j -marginal of $p_{G_k}^{\mathbf{X}}$. For our Gaussian parametrization, using (5), this becomes

$$\begin{aligned} l(\Sigma_{G_1}, \dots, \Sigma_{G_K}; S) &= \\ &- \frac{n}{2} \sum_k \left(|C_k| \log 2\pi + \log \frac{|\Sigma_{G_k}|}{\prod_{j \in \text{pa}(C_k)} \sigma_{kj}^2} + \frac{n-1}{n} \text{tr}(\Sigma_{G_k}^{-1} S_{G_k} - |\text{pa}(C_k)|) \right), \end{aligned}$$

where S_{G_k} is the restriction of S to the rows and columns corresponding to C_k , and σ_{kj}^2 is the diagonal entry of Σ_{G_k} corresponding to parent node j . Note that now the log-likelihood depends on $\{x_i^{(s)}\}$ and $p_G^{\mathbf{X}}$ only via S and $\Sigma_{G_1}, \dots, \Sigma_{G_K}$. Furthermore, the log-likelihood is now a sum of contributions from the submodels G_k . This means we only need to re-compute the likelihood of the submodels that are affected by an edge change when scoring the local neighborhood. In practice, we also cache the submodels scores, that is, we assign each encountered submodel a unique hash and store the respective scores, so they can be re-used.

3.2 Uniformly Random Restarts

To restart the greedy search we need random starting points (BAPs), and it seems desirable to sample them *uniformly* at random⁵. Just like for DAGs, it is not straightforward to achieve this. What is often done in practice (and implemented in the `pcalg` package (Kalisch et al., 2012) as `randomDAG()`) is uniform sampling of triangular (adjacency) matrices and subsequent uniform permutation of the nodes. However, this does not result in uniformly distributed graphs, since for some triangular matrices many permutations

⁵Another motivation for uniform BAP generation is generating ground truths for simulations.

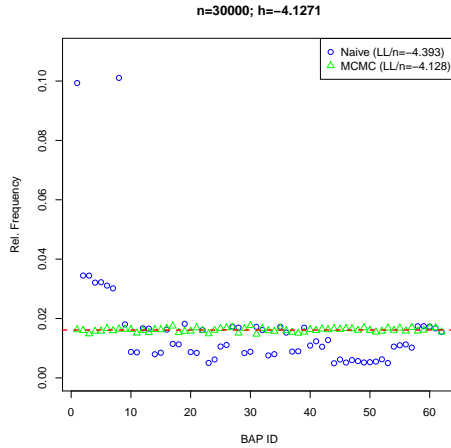


Figure 3: Relative frequencies of the 62 3-node BAPs when sampled 30000 times with the “naive” (triangular matrix sampling) and the MCMC method.

yield the same graph (the empty graph is an extreme example). The consequence is a shift of weight to more symmetric graphs, that are invariant under some permutations of their adjacency matrices. A simple example with BAPs for $d = 3$ is shown in Figure 3. One way around this is to design a random process with graphs as states and a uniform limiting distribution. A corresponding Markov Chain Monte Carlo (MCMC) approach is described for example in Melançon et al. (2001) for the case of DAGs. See also Kuipers and Moffa (2015) for an overview of different sampling schemes.

We adapted this method for BAPs. Specifically, we used the following transition rules: in each step a position (i, j) gets sampled uniformly at random;

- if there is an edge at (i, j) , remove this with probability 0.5;
- if there is no edge at (i, j) :
 - add $i \rightarrow j$ with probability 0.5, as long as this does not create a directed cycle;
 - add $i \leftrightarrow j$ with probability 0.5.

It is easy to check that the resulting transition matrix is irreducible and symmetric and hence the Markov chain has a (unique) uniform stationary distribution. Thus, starting from any graph, after an initial burn-in period, the distribution of the visited states will be approximately uniform over the set of all BAPs. In practice, we start the process from the empty graph and sample after taking $O(d^4)$ steps (c.f. Kuipers and Moffa (2015)).

It is straightforward to adapt this sampling scheme to a number of constraints, for example uniform sampling over all BAPs with a given maximal in-degree.

3.3 Greedy Equivalence Class Construction

We propose the following recursive algorithm to greedily estimate the distributional equivalence class $EC(G)$ of a given BAP G with score ζ . We start by populating the *empirical equivalence class* $\widehat{EC}(G)$ with graphs that have the same skeleton and colliders as G , since these are guaranteed to be equivalent by Theorem 2. This is a significant computational shortcut, since these graphs do not have to be found greedily anymore. Then, starting from G , at each recursion level we search all edge-change neighbors of the current BAP for BAPs that have a score within ϵ of ζ (edge additions or deletions would result in non-equivalent graphs by Theorem 3). For each such BAP, we spark a new recursive search until a maximum depth of $d(d-1)/2$ (corresponding to the maximum number of possible edges) is reached, and always comparing against the original score ζ . Already visited states are stored and ignored. Finally, all found graphs are added to $\widehat{EC}(G)$. The main tuning parameter here is ϵ , essentially specifying the threshold for statistically indistinguishable graphs. This approach of approximating the equivalence class has the advantage of also including neighbouring equivalence classes, that are statistically indistinguishable from the given data, thus being on the conservative side.

3.4 Implementation

Our implementation is done in the statistical computing language R (R Core Team, 2015). The code is available as supplemental material to this paper, and it will also be published in a future version of the R package `pcalg` (Kalisch et al., 2012). We make heavy use of the RICF implementation `fitAncestralGraph()`⁶ in the `ggm` package (Marchetti et al., 2015). We noted that there are sometimes convergence issues, so we adapted the implementation of RICF to include a maximal iteration limit (which we set to 10 by default).

4 Empirical Results

In this section we present some empirical results to show the effectiveness of our method. First, we consider a simulation setting where we can compare against the ground truth. Then we turn to a well known genomic data set, where the ground truth is unknown, but the likelihood of the fitted models can be compared against other methods.

⁶Despite the function name the implementation is not restricted to ancestral graphs.

4.1 Causal Effects Discovery on Simulated Data

To validate our method, we randomly generate ground truths, simulate data from them, and try to recover them from the generated datasets. This procedure is repeated $N = 100$ times and the results are averaged. We now discuss each step in more detail.

Randomly generate a BAP G .

We do this *uniformly* at random (for a fixed model size $d = 10$ and maximal in-degree $\alpha = 2$). The sampling procedure is described in Section 3.2.

Randomly generate a parametrization θ_G .

We sample the directed edge labels in B independently from a standard Normal distribution. We do the same for the bidirected edge labels in Ω , and set the error variances (diagonal entries of Ω) to the respective row-sums of absolute values plus an independently sampled $\chi^2(1)$ value⁷.

Simulate data $\{x_i^{(s)}\}$ from θ_G .

This is straightforward, since we just need to sample from a multivariate Normal distribution with mean $\mathbf{0}$ and covariance $\phi(\theta_G)$. We use the function `rmvnorm()` from the package `mvtnorm` (Genz et al., 2014).

Find an estimate \hat{G} from $\{x_i^{(s)}\}$.

We use greedy search with $R = 100$ uniformly random restarts (as outlined in Section 3) for this, as well as one greedy forward search starting from the empty model.

Compare G and \hat{G} .

This is not so straightforward, since the structure of equivalence classes for BAPs is not known. We therefore make use of the greedy approach described in Section 3.3 with $\epsilon = 10^{-10}$ to get $\widehat{EC}(G)$ and $\widehat{EC}(\hat{G})$.

We proceed by estimating the minimal absolute causal effects E_G^{min} between all nodes over the empirical equivalence class, analogous to the IDA method (Maathuis et al., 2009). Thus, for each graph $G' \in \widehat{EC}(G)$ in the empirical equivalence class with estimated parameters $\hat{\theta}_{G'} = (\hat{B}', \hat{\Omega}')$, we compute the estimated causal effects matrix \hat{E} according to (4). We then take absolute values and take the entry-wise minima over all \hat{E} to obtain \hat{E}_G^{min} . We do the same for \hat{G} to get $\hat{E}_{\hat{G}}^{min}$.

To compare the estimated causal effects of the ground truth G and those of the greedy search result \hat{G} , we treat this as a classification problem, where $(\hat{E}_{\hat{G}}^{min})_{ij}$ is giving a confidence score for the event $(\hat{E}_G^{min})_{ij} > 0$, and we re-

⁷By Gershgorin's circle theorem, this is guaranteed to result in a positive definite matrix. To increase stability, we also repeat the sampling of Ω if its minimal eigenvalue is less than 10^{-6} .

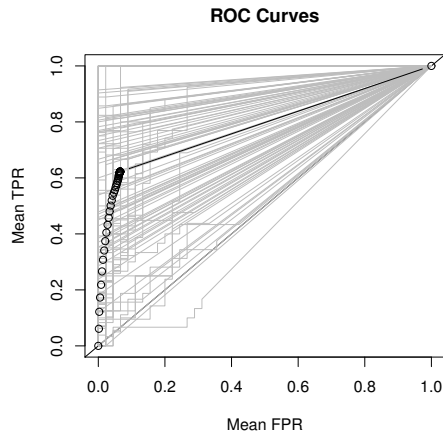


Figure 4: ROC curves for causal effect discovery for $N = 100$ simulation runs of BAPs with $d = 10$ nodes and a maximal in-degree of $\alpha = 2$. Sample size was $n = 1000$, greedy search was repeated $R = 100$ times at uniformly random starting points. The average area under the ROC curves (AUC) is 0.78. The thick curve is the point-wise average of the individual ROC curves.

port the area under the ROC curve (AUC, see Hanley and McNeil (1983)). The AUC ranges from 0 to 1, with 1 meaning perfect classification and 0.5 being equivalent to random guessing⁸.

The results can be seen in Figure 4 with an AUC of 0.78. While this suggests that perfect graph discovery is usually not achieved, causal effects (which are often more relevant in practice) can be identified to some extent. The computations took 2.5 hours on an AMD Opteron 6174 processor using 20 cores.

4.2 Genomic Data

We also applied our method to a well-known genomics data set (Sachs et al., 2005), where the expression of 11 proteins in human T-cells was measured under 14 different experimental conditions. There are likely hidden confounders, which makes this setting suitable for hidden variable models. However, it is questionable whether the bow-freeness, linearity, and Gaussianity assumptions hold to a reasonable approximation (in fact the data seem not multivariate Normal). Furthermore, there does not exist a ground truth

⁸A bit of care has to be taken because of the fact that the cases $(\hat{E}_G^{min})_{ij} > 0$ and $(\hat{E}_G^{min})_{ji} > 0$ exclude each other, but we took this into account when computing the false positive rate.

network (although some individual links between pairs of proteins are reported as known in the original paper). So we abstain from presenting a “best” network, but instead compare the model fit of BAPs and DAGs from a purely statistical point of view.

To do this, we first log-transform all variables since they are heavily skewed. We then run two sets of greedy searches for each of the 14 data sets: one with BAPs and one with DAGs. For the BAPs we use 100 and for the DAGs we use 1000 random restarts (DAG models can be fit much faster than BAP models). The results for datasets 1 to 8 can be seen in Figure 5⁹. The penalized likelihood scores of the best BAP models are always much higher than the corresponding scores for the DAG models, despite the larger number of random restarts for the DAGs. Furthermore, while there is a marked improvement from the random starting scores for BAPs, the improvement for the DAG scores is marginal. For these datasets, BAPs seem to be superior to DAGs in modelling the data. The computations took 4 hours for the BAP models and 1.5 hours for the DAG models on an AMD Opteron 6174 processor using 20 cores.

5 Conclusions

We have presented a structure learning method for BAPs, which can be viewed as a generalization of Gaussian linear DAG models that allow for certain latent variables. Our method is computationally feasible and the first of its kind. The results on simulated data are promising, keeping in mind that structure learning and inferring causal effects are difficult, even for the easier case with DAGs. The main sources of errors (given the model assumptions are fulfilled) are sampling variability, finding a local optimum only, and not knowing the equivalence classes. Local optima are a general weakness of many structure learning methods in Bayesian networks since this problem is NP-hard in general (Chickering, 1996). In our simulations, overestimating the equivalence class leads to too few causal effects, while the opposite happens if we underestimate it. On the other hand, our approach of greedily approximating the empirical equivalence class is building on the idea that some models are statistically indistinguishable, due to limited sample size and estimation error. Therefore, our approach has the advantage that it can include neighboring equivalence classes, that score almost as well, which is desirable from a statistical point of view. Our theoretical results about model equivalence go some way towards characterizing the distributional equivalence classes in BAP models and allow us to efficiently approximate them empirically.

In many applications, not all relevant variables are observed, so allowing for hidden variables in the model should improve both the statistical fit as

⁹The results for the other 6 datasets are qualitatively similar.

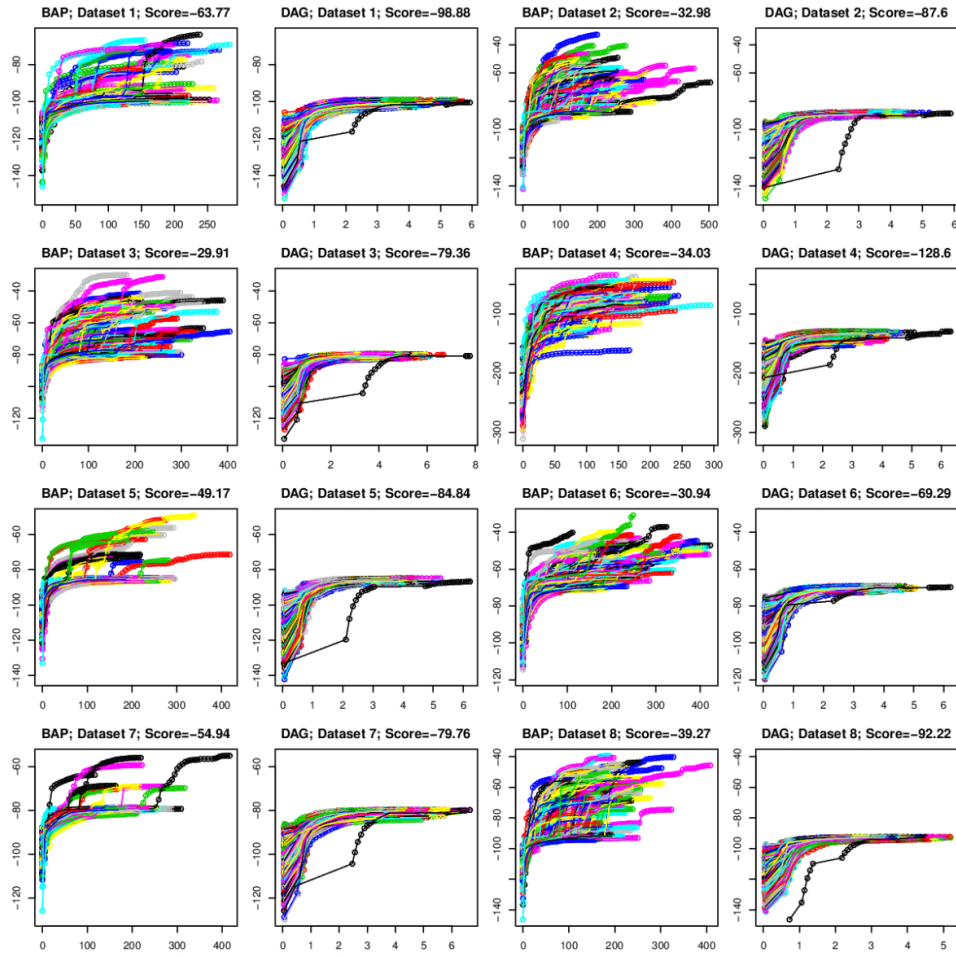


Figure 5: Greedy search runs on the first 8 of 14 genomic datasets with BAPs and DAGs. The x-axis is time in seconds, the y-axis is the (normalized) penalized likelihood score. Each path corresponds to a run of a greedy search with a different random restart, with each point on the path being a state visited by this greedy search run.

well as the interpretability in these cases. The former could be confirmed by applying our method to some real datasets. When comparing our method with traditional DAG models, that do not allow for hidden variables, we could demonstrate a marked improvement of the likelihood scores.

A Appendix

A.1 Distributional Equivalence

We first make precise the definition of an important class of paths: *treks*. These are paths that do not contain colliders. We adopt the notation of Foygel et al. (2012). A trek τ from i to j can have one of the following forms:

$$v_l^L \leftarrow \cdots \leftarrow v_0^L \longleftrightarrow v_0^R \rightarrow \cdots \rightarrow v_r^R$$

or

$$v_l^L \leftarrow \cdots \leftarrow v_0 \rightarrow \cdots \rightarrow v_r^R,$$

where $v_l^L = i$ and $v_r^R = j$ and in the second case $v_0 = v_0^L = v_0^R$. Accordingly, we define the *left-hand side* of τ as $\text{Left}(\tau) = v_l^L \leftarrow \cdots \leftarrow v_0^L$ and the *right-hand side* of τ as $\text{Right}(\tau) = v_0^R \rightarrow \cdots \rightarrow v_r^R$. Note that there is nothing inherently directional about a trek other than the (arbitrary) definition which end node is on the left. That is, every trek from i to j is also a trek from j to i just with the left and right sides switched. We denote the lengths of the left- and right-hand sides of a trek τ by $\lambda_L(\tau)$ and $\lambda_R(\tau)$ respectively. If τ does not contain a bidirected edge, we define its *head* to be $H_\tau = v_0$, otherwise $H_\tau = \emptyset$. If the left- and right-hand sides of τ do not intersect (except possibly at H_τ), we call τ *simple*¹⁰. We define the following sets that will be useful later:

$$\mathcal{D}_G^{ij} = \{\pi \mid \pi \text{ is a directed path from } i \text{ to } j \text{ in } G\},$$

$$\mathcal{T}_G^{ij} = \{\tau \mid \tau \text{ is a trek from } i \text{ to } j \text{ in } G\},$$

$$\mathcal{S}_G^{ij} = \{\tau \mid \tau \text{ is a simple trek from } i \text{ to } j \text{ in } G\}.$$

We will usually drop the subscript if it is clear from context which is the reference graph.

We now show some intermediate results that are well-known, but we prove them here for completeness nevertheless. All of these apply more generally to path diagrams (possibly cyclic and with bows).

Lemma 1. *Let $B \in \mathbb{R}^{d \times d}$ such that every eigenvalue λ of B satisfies $|\lambda| < 1$. Then $(I - B)^{-1}$ exists and is equal to $\sum_{s=0}^{\infty} B^s$.*

¹⁰Note that each side might well be self-intersecting, if the corresponding graph is cyclic.

Proof. First note that $\det(\lambda I - B) = 0$ only if $|\lambda| < 1$, hence $\det(I - B) \neq 0$, and therefore $(I - B)^{-1}$ exists. The eigenvalue condition also implies $\lim_{l \rightarrow \infty} B^l = 0$, therefore

$$(I - B) \sum_{s=0}^{\infty} B^s = \lim_{l \rightarrow \infty} \sum_{s=0}^l (B^s - B^{s+1}) = \lim_{l \rightarrow \infty} (I - B^{l+1}) = I,$$

and the result follows. \square

Lemma 2. *Let G be a path diagram over d nodes and $B \in \mathcal{B}_G$. Then*

$$(B^l)_{ij} = \sum_{\substack{\pi \in \mathcal{D}^{ji} \\ \lambda(\pi) = l}} \prod_{s \rightarrow t \in \pi} B_{ts}.$$

Proof. By induction on l . For $l = 1$ the claim follows from the definition of \mathcal{B}_G . Using the inductive hypothesis we get

$$(B^l)_{ij} = (BB^{l-1})_{ij} = \sum_{k=1}^d B_{ik} (B^{l-1})_{kj} = \sum_{k=1}^d B_{ik} \sum_{\substack{\pi \in \mathcal{D}^{jk} \\ \lambda(\pi) = l-1}} \prod_{s \rightarrow t \in \pi} B_{ts},$$

and the claim follows, since every directed path from j to i of length l can be decomposed into a directed path π of length $l - 1$ from j to some node k and the edge $k \rightarrow i$. \square

Lemma 3. *Let G be an acyclic path diagram over d nodes and $B \in \mathcal{B}_G$. Then $(I - B)^{-1} = I + B + \dots + B^{d-1}$.*

Proof. Since G is acyclic, there is an ordering of the nodes, such that B is strictly lower triangular and hence all its eigenvalues are zero. Furthermore, the longest directed path in G has length $d - 1$. Therefore the result follows from Lemma 1 and Lemma 2. \square

The following theorem is a version of Wright's theorem that applies to non-standardized variables. It does not require a proper parametrization (in the sense that Ω needs to be positive definite).

Theorem 4. *Let G be a (possibly cyclic) path diagram over d nodes, $B \in \mathcal{B}_G$, and $\Omega \in \mathbb{R}^{d \times d}$ such that Ω is symmetric (but not necessarily positive definite) and $\Omega_{ij} = 0$ if $i \leftrightarrow j$ is not an edge in G . Then the entries of the matrix $\phi = (I - B)^{-1} \Omega (I - B)^{-T}$ are given by*

$$\begin{aligned} \phi_{ij} &= \sum_{\substack{\tau \in \mathcal{S}^{ij} \\ \leftrightarrow \in \tau}} \prod_{s \rightarrow t \in \tau} B_{ts} \prod_{s \leftrightarrow t \in \tau} \Omega_{st} + \sum_{\substack{\tau \in \mathcal{S}^{ij} \\ \leftrightarrow \notin \tau}} \prod_{s \rightarrow t \in \tau} B_{ts} \cdot \phi_{H_\tau H_\tau} \quad (i \neq j), \\ \phi_{ii} &= \sum_{\substack{\tau \in \mathcal{T}^{ii} \\ \leftrightarrow \in \tau}} \prod_{s \rightarrow t \in \tau} B_{ts} \prod_{s \leftrightarrow t \in \tau} \Omega_{st} + \sum_{\substack{\tau \in \mathcal{T}^{ii} \\ \leftrightarrow \notin \tau}} \prod_{s \rightarrow t \in \tau} B_{ts} \cdot \Omega_{H_\tau H_\tau} + \Omega_{ii}. \end{aligned}$$

Proof. Let us write

$$c_e(\tau; B, \Omega) = \prod_{s \rightarrow t \in \tau} B_{ts} \prod_{s \leftrightarrow t \in \tau} \Omega_{st}$$

as a shorthand for the edge contribution¹¹ of a trek τ given parameter matrices B and Ω . We write $c(\tau; B, \Omega) = c_e(\tau; B, \Omega) \cdot \Omega_{H_\tau H_\tau}$ for the total contribution of τ (where we define $\Omega_{H_\tau H_\tau}$ to be 1 if τ contains a bidirected edge and therefore $H_\tau = \emptyset$).

Using Lemma 1, we can expand ϕ as $\phi = \sum_{k=0}^{\infty} \sum_{l=0}^{\infty} B^k \Omega (B^l)^T$. We now first show the following intermediate result, which interprets the entries of these matrices as contributions of certain treks:

$$(B^k \Omega (B^l)^T)_{ij} = \sum_{\substack{\tau \in \mathcal{T}^{ij} \\ \lambda_L(\tau)=k \\ \lambda_R(\tau)=l}} c(\tau; B, \Omega) + \Omega_{ii} \mathbb{1}\{i = j\}, \quad (8)$$

for integers $k \geq 0$, $l \geq 0$. To see this, we expand the double matrix product and use Lemma 2 to get

$$\begin{aligned} (B^k \Omega (B^l)^T)_{ij} &= \sum_{a=1}^d \sum_{b=1}^d (B^k)_{ia} \Omega_{ab} (B^l)_{jb} \\ &= \sum_{a=1}^d \sum_{b=1}^d \left(\sum_{\substack{\pi \in \mathcal{D}^{ai} \\ \lambda(\pi)=k}} \prod_{s \rightarrow t \in \pi} B_{ts} \right) \Omega_{ab} \left(\sum_{\substack{\pi \in \mathcal{D}^{bj} \\ \lambda(\pi)=l}} \prod_{s \rightarrow t \in \pi} B_{ts} \right), \end{aligned}$$

and (8) follows since each bracketed expression corresponds to one side of the trek from i to j via a and b (and the diagonal entries of Ω do not correspond to a trek, so they are separate). Now summing over k and l gives the following

$$\phi_{ij} = \sum_{\tau \in \mathcal{T}^{ij}} c(\tau; B, \Omega) + \Omega_{ii} \mathbb{1}\{i = j\}, \quad (9)$$

which gives the result for the diagonal entries ϕ_{ii} .

For the off-diagonal entries ϕ_{ij} , we can get a simpler expression involving only simple treks and the diagonal entries ϕ_{ii} . Note that every trek τ can be uniquely decomposed into a simple part $\xi(\tau)$ and a (possibly empty) non-simple part $\rho(\tau)$ (we just split at the point, where the right- and the left-hand sides of τ first intersect). Since

$$c(\tau) = \begin{cases} c_e(\xi(\tau)) \cdot \Omega_{H_{\xi(\tau)} H_{\xi(\tau)}} & \text{if } \rho(\tau) = \emptyset \\ c_e(\xi(\tau)) \cdot c(\rho(\tau)) & \text{otherwise,} \end{cases}$$

¹¹That is, the contribution depending only on the edge labels and not the diagonal elements of Ω .

(dropping the parameter matrices B and Ω in our notation), we can factor out the contributions of the simple parts. Note that if the simple part $\xi(\tau)$ contains a bidirected edge, then $\rho(\tau)$ must be empty and $\Omega_{H_\xi(\tau)H_\xi(\tau)} = 1$. Hence (9) becomes

$$\begin{aligned}
\phi_{ij} &= \sum_{\substack{\tau \in \mathcal{T}^{ij} \\ \leftrightarrow \in \xi(\tau)}} c(\tau) + \sum_{\substack{\tau \in \mathcal{T}^{ij} \\ \leftrightarrow \notin \xi(\tau) \\ \rho(\tau) \neq \emptyset}} c(\tau) + \sum_{\substack{\tau \in \mathcal{T}^{ij} \\ \leftrightarrow \notin \xi(\tau) \\ \rho(\tau) = \emptyset}} c(\tau) \\
&= \sum_{\substack{\tau \in \mathcal{T}^{ij} \\ \leftrightarrow \in \xi(\tau)}} c_e(\xi(\tau)) + \sum_{\substack{\tau \in \mathcal{T}^{ij} \\ \leftrightarrow \notin \xi(\tau) \\ \rho(\tau) \neq \emptyset}} c_e(\xi(\tau)) \cdot c(\rho(\tau)) + \sum_{\substack{\tau \in \mathcal{T}^{ij} \\ \leftrightarrow \notin \xi(\tau) \\ \rho(\tau) = \emptyset}} c_e(\xi(\tau)) \cdot \Omega_{H_\xi(\tau)H_\xi(\tau)} \\
&= \sum_{\substack{\xi \in \mathcal{S}^{ij} \\ \leftrightarrow \in \xi}} c_e(\xi) + \sum_{\substack{\xi \in \mathcal{S}^{ij} \\ \leftrightarrow \notin \xi}} c_e(\xi) \sum_{\rho \in \mathcal{T}^{H_\xi H_\xi}} c(\rho) + \sum_{\substack{\xi \in \mathcal{S}^{ij} \\ \leftrightarrow \notin \xi}} c_e(\xi) \cdot \Omega_{H_\xi H_\xi} \\
&= \sum_{\substack{\xi \in \mathcal{S}^{ij} \\ \leftrightarrow \in \xi}} c_e(\xi) + \sum_{\substack{\xi \in \mathcal{S}^{ij} \\ \leftrightarrow \notin \xi}} c_e(\xi) \left(\sum_{\rho \in \mathcal{T}^{H_\xi H_\xi}} c(\rho) + \Omega_{H_\xi H_\xi} \right),
\end{aligned}$$

and the result follows. \square

The following version for standardized parameters is often quoted as Wright's theorem.

Theorem 5. *Let G be a (not necessarily acyclic) path diagram over d nodes, $B \in \mathcal{B}_G$, and $\Omega \in \mathbb{R}^{d \times d}$ such that Ω is symmetric (but not necessarily positive definite) and $\Omega_{ij} = 0$ if $i \leftrightarrow j$ is not an edge in G . Furthermore assume that we have standardized parameters B, Ω such that $(\phi(B, \Omega))_{ii} = 1$ for all i . Then the off-diagonal entries of $\phi(B, \Omega)$ are given by*

$$(\phi(B, \Omega))_{ij} = \sum_{\tau \in \mathcal{S}^{ij}} \prod_{s \rightarrow t \in \tau} B_{ts} \prod_{s \leftrightarrow t \in \tau} \Omega_{st}.$$

Proof. This is a direct consequence of Theorem 4. \square

We can now prove Theorem 2, which is a consequence of Wright's formula.

Proof of Theorem 2. Let $\theta_{G_1} \in \bar{\Theta}_{G_1}$ and choose $\theta_{G_2} = (B_2, \Omega_2)$ such that their edge labels agree, that is,

$$(B_2)_{ij} = \begin{cases} (B_1)_{ij} & \text{if } i \leftarrow j \in G_1, i \leftarrow j \in G_2, \\ (\Omega_1)_{ij} & \text{if } i \leftrightarrow j \in G_1, i \leftarrow j \in G_2, \\ 0 & \text{if } i \leftarrow j \notin G_2, \end{cases}$$

and

$$(\Omega_2)_{ij} = \begin{cases} (B_1)_{ij} & \text{if } i \leftarrow j \in G_1, i \leftrightarrow j \in G_2, \\ (\Omega_1)_{ij} & \text{if } i \leftrightarrow j \in G_1, i \leftrightarrow j \in G_2, \\ 0 & \text{if } i \leftrightarrow j \notin G_2. \end{cases}$$

This is possible since G_1 and G_2 have the same skeleton: we just assign the edge labels of G_1 to G_2 , irrespective of the edge type. The diagonal entries of Ω_2 are still free—we now show that they can be used to enforce

$$(\phi(B_2, \Omega_2))_{ii} = 1 \tag{10}$$

for all i , which defines a linear system for the diagonal entries of Ω_2 . Let $\mathbf{d} = \text{diag}(\Omega_2)$ be the vector consisting of the diagonal elements of Ω_2 , and write (10) as $M\mathbf{d} = \mathbf{1}$, where M is the coefficient matrix of the linear system. To show that (10) always has a solution, we need to show that $\det(M) \neq 0$. Without loss of generality, assume that the nodes are topologically ordered according to G_2 (this is possible since G_2 is assumed to be acyclic), that is, there is no directed path from i to j if $i > j$. Then we have $H_\tau < i$ (or $H_\tau = \emptyset$) for all $\tau \in \mathcal{T}^{ii}$, and using the expression for ϕ_{ii} in Theorem 4 we see that M must be lower triangular with diagonal equal to 1. Thus $\det(M) = 1$, and we can enforce (10).

Since G_1 and G_2 share the same collider structure, the sets of simple treks between any two nodes are the same in both graphs: $\mathcal{S}_{G_1}^{ij} = \mathcal{S}_{G_2}^{ij} \forall i, j$. Together with Theorem 5 and the fact that the edge labels agree this shows that

$$\phi(\theta_{G_1}) = \phi(\theta_{G_2}). \tag{11}$$

What is left to show is that Ω_2 is a valid covariance matrix, that is, it is positive semi-definite. By (3) and (11) we have that

$$\Omega_2 = (I - B_2)\Sigma_1(I - B_2)^T,$$

where $\Sigma_1 = \phi(\theta_{G_1})$. Since Σ_1 is positive semidefinite, so is Ω_2 . \square

Finally, we come to the proof of Theorem 3, which uses the fact that ϕ is injective on the identifiable parameter space (and the non-identifiable part has measure zero).

Proof of Theorem 3. We show that G_1 and G_2 are not distributionally equivalent by showing that their covariance sets are not equal, i.e. that $\phi(\bar{\Theta}_{G_1}) \neq \phi(\bar{\Theta}_{G_2})$ (see Definition 1). By assumption, the set of edges in G_1 must be a strict subset of the set of edges in G_2 . This implies $\bar{\Theta}_{G_1} \subset \bar{\Theta}_{G_2}$ and therefore $\phi(\bar{\Theta}_{G_1}) \subseteq \phi(\bar{\Theta}_{G_2})$. It is left to show that the subset relation is strict. To see this, we first partition the parameter spaces $\bar{\Theta}_{G_i}$ into

the identifiable and the non-identifiable parts: $\bar{\Theta}_{G_i} = \tilde{\Theta}_{G_i} \dot{\cup} \Theta_{G_i}^0$, where $\tilde{\Theta}_{G_i} := \{\theta \in \bar{\Theta}_{G_i} \mid \theta \text{ is identifiable}\}$, $\Theta_{G_i}^0 := \bar{\Theta}_{G_i} \setminus \tilde{\Theta}_{G_i}$ (and we use the notation $A = B \dot{\cup} C$ to express A as a union of disjoint sets B and C). This yields $\phi(\bar{\Theta}_{G_i}) = \phi(\tilde{\Theta}_{G_i}) \dot{\cup} \phi(\Theta_{G_i}^0)$, where the fact that they are disjoint follows from Definition 1. We trivially have $\Theta_{G_1}^0 \subseteq \Theta_{G_2}^0$ and therefore $\phi(\Theta_{G_1}^0) \subseteq \phi(\Theta_{G_2}^0)$. Assume for the moment, that the following holds:

$$\tilde{\Theta}_{G_1} \subset \tilde{\Theta}_{G_2}. \quad (12)$$

Then, since ϕ is (by definition) injective on $\tilde{\Theta}_{G_2} \supseteq \tilde{\Theta}_{G_1}$, we also have $\phi(\tilde{\Theta}_{G_1}) \subset \phi(\tilde{\Theta}_{G_2})$, and hence $\phi(\bar{\Theta}_{G_1}) \subset \phi(\bar{\Theta}_{G_2})$, which proves the claim.

The rest of the proof is a technical argument to show that the subset relation (12) is actually strict. This is trivial for the normalized parameters $\bar{\Theta}_{G_i}$, but the case of the identifiable parameters $\tilde{\Theta}_{G_i}$ requires a bit of care. We use a measure-theoretic argument for this, using the fact that the difference between $\bar{\Theta}_{G_i}$ and $\tilde{\Theta}_{G_i}$ has measure zero. Let μ_m be the m -dimensional Lebesgue measure on the Cartesian space \mathbb{R}^e (for any positive integer e). Let e_i be the number of edges in G_i . We now show that

$$\mu_{e_2}(\xi(\tilde{\Theta}_{G_1})) \neq \mu_{e_2}(\xi(\tilde{\Theta}_{G_2})), \quad (13)$$

where ξ is a suitable vectorization of the parametrizations θ (see below). This means $\tilde{\Theta}_{G_1} \neq \tilde{\Theta}_{G_2}$ and hence implies (12).

Let $\xi : \mathbb{R}^{d \times d} \times \mathbb{R}^{d \times d} \rightarrow \mathbb{R}^{3\binom{d}{2}}$ be the vectorized version of the possible edge weights for parametrizations $\theta_{G_i} = (B, \Omega)$. That is, $\xi(\theta_{G_i})$ is the concatenation of the off-diagonal entries of B (directed edges) and the strictly lower-triangular part of Ω (bidirected edges). Note that the error variances (diagonal of Ω) are left out in the vectorization, but ξ is still injective on $\bar{\Theta}_{G_i}$, since the diagonal of Ω is determined by the normalization constraint $\Sigma_{ii} = 1$ (it is equal to the diagonal of $(I - B)\Sigma(I - B)^T$, where $\Sigma_{ii} = 1$, and Σ_{ij} ($i \neq j$) are determined by $\xi(B, \Omega)$ via Theorem 5). Furthermore, $\xi(\Theta_{G_i})$ is isomorphic to a subset of \mathbb{R}^{e_i} , since only e_i of its $3\binom{d}{2}$ coordinates will be non-zero.

The injectivity property implies $\xi(\bar{\Theta}_{G_2}) = \xi(\Theta_{G_2}^0 \dot{\cup} \tilde{\Theta}_{G_2}) = \xi(\Theta_{G_2}^0) \dot{\cup} \xi(\tilde{\Theta}_{G_2})$. Brito and Pearl (2002) showed that $\mu_{e_2}(\xi(\Theta_{G_2}^0)) = 0$, hence $\mu_{e_2}(\xi(\bar{\Theta}_{G_2})) = \mu_{e_2}(\xi(\tilde{\Theta}_{G_2}))$. On the other hand, it is easy to see that $\mu_{e_2}(\xi(\tilde{\Theta}_{G_1})) = 0$, since $\xi(\tilde{\Theta}_{G_1})$ is isomorphic to a subset of \mathbb{R}^{e_1} and $e_1 < e_2$. We therefore need to show $\mu_{e_2}(\xi(\bar{\Theta}_{G_2})) > 0$ in order to prove (13). Our argument for this is that the set $\xi(\bar{\Theta}_{G_2})$ is of essentially the same size as \mathbb{R}^{e_2} , the only restriction being the positive-definiteness of the error covariance matrices Ω which cuts out a subset of measure zero.

Let ξ_{G_2} be the restriction of ξ to the entries that correspond to edges in G_2 . Then $\xi_{G_2}(\Theta_{G_2}) \subset \mathbb{R}^{e_2}$, and $\mu_{e_2} \circ \xi$ and $\mu_{e_2} \circ \xi_{G_2}$ are equal for all (measurable) subsets of Θ_{G_2} . Note that ξ_{G_2} is not injective on Θ_{G_2} , since

the error variances are ignored. But instead of the inverse $\xi_{G_2}^{-1}$ we can work with the following construction. Let $\nu(v)$ be the unique element of $\xi_{G_2}^{-1}(v)$ that is normalized, i.e. such that $(\phi(\nu(v)))_{ii} = 1$ (this is the same as for the injectivity argument for ξ on $\bar{\Theta}_{G_i}$ above). Then ν^{-1} and ξ_{G_2} are identically equal on $\bar{\Theta}_{G_2}$. Consider the set

$$\begin{aligned}\mathbb{R}^{e_2} \setminus \nu^{-1}(\bar{\Theta}_{G_2}) &= \{v \in \mathbb{R}^{e_2} \mid \nu(v) \notin \bar{\Theta}_{G_2}\} \\ &= \{v \in \mathbb{R}^{e_2} \mid \phi(\nu(v)) \text{ is not positive definite}\} \\ &= \{v \in \mathbb{R}^{e_2} \mid \exists l \text{ such that } f_l(\phi(\nu(v))) = 0\},\end{aligned}$$

where f_l is the determinant of the l -th leading principal minor. Since ν , ϕ , and f_l all are polynomial functions, the set is a polynomial equality constrained subset of \mathbb{R}^{e_2} . According to Okamoto (1973) such sets have Lebesgue measure zero, that is, $\mu_{e_2}(\mathbb{R}^{e_2} \setminus \nu^{-1}(\bar{\Theta}_{G_2})) = 0$, and therefore $0 < \mu_{e_2}(\mathbb{R}^{e_2}) = \mu_{e_2}(\nu^{-1}(\bar{\Theta}_{G_2})) = \mu_{e_2}(\xi_{G_2}(\bar{\Theta}_{G_2})) = \mu_{e_2}(\xi(\bar{\Theta}_{G_2}))$. This completes the proof. \square

A.2 Likelihood Separation

Since we can write $\epsilon = \epsilon(\mathbf{X})$ as a function of $\mathbf{X} = (X_1, \dots, X_d)$, we have that their densities satisfy

$$p_G^{\mathbf{X}}(X_1, \dots, X_d) = p_G^\epsilon(\epsilon_1(\mathbf{X}), \dots, \epsilon_d(\mathbf{X})). \quad (14)$$

The joint density for the errors ϵ can be factorized according to the independence structure implied by Ω . Let us adopt the notation $\{X\}_I := \{X_i\}_{i \in I}$ and $\{\epsilon\}_I := \{\epsilon_i\}_{i \in I}$ for some index set I . Then we have $\{\epsilon\}_{C_k} \perp\!\!\!\perp \{\epsilon\}_{C_l} \forall k \neq l$. Furthermore, we implicitly refer to marginalized densities via the arguments, i.e. we write $p_G^\epsilon(\{\epsilon\}_{C_1})$ for the marginal density of $\{\epsilon\}_{C_1}$. We can thus write

$$p_G^\epsilon(\epsilon_1, \dots, \epsilon_d) = p_G^\epsilon(\{\epsilon\}_{C_1}) \cdots p_G^\epsilon(\{\epsilon\}_{C_K}).$$

Hence (14) becomes

$$p_G^{\mathbf{X}}(X_1, \dots, X_d) = \prod_k p_G^\epsilon \left(\left\{ X_i - \sum_{j \in \text{pa}(i)} B_{ij} X_j \right\}_{i \in C_k} \right). \quad (15)$$

Each factor depends only on the nodes in the respective component C_k and the parents of that component $\text{pa}(C_k)$. By the same argument the joint density of the submodel G_k is

$$\begin{aligned}p_{G_k}^{\mathbf{X}}(\{X\}_{V_k}) &= p_{G_k}^\epsilon(\{\epsilon\}_{C_k}) \prod_{j \in \text{pa}(C_k)} p_{G_k}^\epsilon(\epsilon_j) \\ &= p_{G_k}^\epsilon \left(\left\{ X_i - \sum_{j \in \text{pa}(i)} B_{ij} X_j \right\}_{i \in C_k} \right) \prod_{j \in \text{pa}(C_k)} p_{G_k}^\epsilon(X_j).\end{aligned}$$

This factorization is symbolic, since the parents $\{X_j\}_{j \in \text{pa}(C_k)}$ will not be independent in general. This does not matter, however, since these terms cancel when reconstructing the full density $p_G^{\mathbf{X}}(X_1, \dots, X_d)$ later. The advantage of this symbolic factorization is that we can still *fit* the (wrong) submodel and then use the easier to compute product of marginal densities to reconstruct the full density, rather than doing the same with the actual submodel factorization and the joint density of the component parents.

Note that

$$p_{G_k}^\epsilon \left(\left\{ X_i - \sum_{j \in \text{pa}(i)} B_{ij} X_j \right\}_{i \in C_k} \right) = p_G^\epsilon \left(\left\{ X_i - \sum_{j \in \text{pa}(i)} B_{ij} X_j \right\}_{i \in C_k} \right),$$

that is, the conditionals $\{X\}_{C_k} | \{X\}_{\text{pa}(C_k)}$ are the same in models G and G_k . This is because the structural equations of $\{X\}_{C_k}$ are the same in these models. Note also that $p_{G_k}^\epsilon(X_j) = p_{G_k}^{\mathbf{X}}(X_j)$ for all $j \in \text{pa}(G_k)$ and all k , since $\text{pa}(C_k)$ are source nodes in model G_k (all edges between them were removed).

Thus we can reconstruct the full joint density (15) from joint densities of the connected component submodels and marginal densities of the parent variables:

$$p_G^{\mathbf{X}}(X_1, \dots, X_d) = \prod_k p_{G_k}^{\mathbf{X}}(\{X\}_{V_k}) \cdot \left(\prod_{j \in \text{pa}(C_k)} p_{G_k}^{\mathbf{X}}(X_j) \right)^{-1}.$$

Writing \mathcal{D} for the observed data $\{x_i^s\}$ (with $1 \leq i \leq d$ and $1 \leq s \leq n$), the log-likelihood can then be written as

$$\begin{aligned} l(p_G^{\mathbf{X}}; \mathcal{D}) &= \sum_{s=1}^n \log p_G^{\mathbf{X}}(x_1^{(s)}, \dots, x_p^{(s)}) \\ &= \sum_{s=1}^n \sum_k \left(\log p_{G_k}^{\mathbf{X}}(\{x_i^{(s)}\}_{i \in V_k}) - \sum_{j \in \text{pa}(C_k)} \log p_{G_k}^{\mathbf{X}}(x_j^{(s)}) \right) \\ &= \sum_k \left(l(p_{G_k}^{\mathbf{X}}; \{x_i^{(s)}\}_{i \in V_k}^{s=1, \dots, n}) - \sum_{j \in \text{pa}(C_k)} l(p_{G_k}^{\mathbf{X}}; \{x_j^{(s)}\}^{s=1, \dots, n}) \right), \end{aligned}$$

where $l(p_{G_k}^{\mathbf{X}}; \{x_j^{(s)}\}^{s=1, \dots, n})$ refers to the likelihood of the X_j -marginal of $p_{G_k}^{\mathbf{X}}$.

References

Brito, C. and Pearl, J. A new identification condition for recursive models with correlated errors. *Structural Equation Modeling*, 9(4):459–474, 2002.

- Chickering, D. M. Learning Bayesian networks is NP-complete. In *Learning from Data*, volume 112 of *Lecture Notes in Statistics*, pages 121–130. 1996.
- Chickering, D. M. Optimal structure identification with greedy search. *Journal of Machine Learning Research*, 3:507–554, 2002.
- Claassen, T., Mooji, J. M., and Heskes, T. Learning sparse causal models is not NP-hard. In *Proceedings of the Twenty-Ninth Conference Annual Conference on Uncertainty in Artificial Intelligence (UAI-13)*, pages 172–181, 2013.
- Colombo, D., Maathuis, M. H., Kalisch, M., and Richardson, T. S. Learning high-dimensional directed acyclic graphs with latent and selection variables. *The Annals of Statistics*, 40(1):294–321, 2012.
- Drton, M., Eichler, M., and Richardson, T. S. Computing maximum likelihood estimates in recursive linear models with correlated errors. *Journal of Machine Learning Research*, 10:2329–2348, 2009.
- Drton, M., Foygel, R., and Sullivant, S. Global identifiability of linear structural equation models. *The Annals of Statistics*, 39(2):865–886, 2011.
- Duncan, O. T. *Introduction to Structural Equation Research*. Academic Press, 1975.
- Evans, R. J. Graphs for margins of bayesian networks. 2014. URL <http://arxiv.org/abs/1408.1809>. Preprint.
- Foygel, R., Draisma, J., and Drton, M. Half-trek criterion for generic identifiability of linear structural equation models. *The Annals of Statistics*, 40(3):1682–1713, 2012.
- Genz, A., Bretz, F., Miwa, T., Mi, X., Leisch, F., Scheipl, F., and Hothorn, T. *mvtnorm: Multivariate Normal and t Distributions*, 2014. URL <http://CRAN.R-project.org/package=mvtnorm>. R package version 1.0-2.
- Glymour, C. and Scheines, R. Causal modeling with the TETRAD program. *Synthese*, 68(1):37–63, 1986.
- Hanley, J. A. and McNeil, B. J. A method of comparing the areas under receiver operating characteristic curves derived from the same cases. *Radiology*, 148(3):839–843, 1983.
- Jöreskog, K. G. A general method for analysis of covariance structures. *Biometrika*, 57(2):239–251, 1970.
- Jöreskog, K. G. *LISREL 8: User's Reference Guide*. Scientific Software International, 2001.

- Kalisch, M., Mächler, M., Colombo, D., Maathuis, M. H., and Bühlmann, P. Causal inference using graphical models with the R package pcalg. *Journal of Statistical Software*, 47(11), 2012.
- Kuipers, J. and Moffa, G. Uniform random generation of large acyclic digraphs. *Statistics and Computing*, 25(2):227–242, 2015.
- Maathuis, M. H., Kalisch, M., and Bühlmann, P. Estimating high-dimensional intervention effects from observational data. *The Annals of Statistics*, 37(6A):3133–3164, 2009.
- Maathuis, M. H., Colombo, D., Kalisch, M., and Bühlmann, P. Predicting causal effects in large-scale systems from observational data. *Nature Methods*, 7(4), 2010.
- Marchetti, G. M., Drton, M., and Sadeghi, K. *ggm: Functions for graphical Markov models*, 2015. URL <http://CRAN.R-project.org/package=ggm>. R package version 2.3.
- Mardia, K. V., Kent, J. T., and Bibby, J. M. *Multivariate Analysis*. Academic Press, 1979.
- Melançon, G., Dutout, I., and Bousquet-Mélou, M. Random generation of directed acyclic graphs. *Electronic Notes in Discrete Mathematics*, 10: 202–207, 2001.
- Okamoto, M. Distinctness of the eigenvalues of a quadratic form in a multivariate sample. *The Annals of Statistics*, 1(4):763–765, 1973.
- Pearl, J. *Causality*. Cambridge University Press, 2000.
- R Core Team. *R: A Language and Environment for Statistical Computing*. R Foundation for Statistical Computing, Vienna, Austria, 2015. URL <http://www.R-project.org/>.
- Richardson, T. A factorization criterion for acyclic directed mixed graphs. In *Proceedings of the Twenty-Fifth Conference on Uncertainty in Artificial Intelligence (UAI-09)*, 2009.
- Richardson, T. and Spirtes, P. Ancestral graph markov models. *The Annals of Statistics*, 30(4):962–1030, 2002.
- Sachs, K., Perez, O., Pe’er, D., Lauffenburger, D. A., and Nolan, G. P. Causal protein-signaling networks derived from multiparameter single-cell data. *Science*, 308(5721):523–529, 2005.
- Shpitser, I., Richardson, T. S., Robins, J. M., and Evans, R. Parameter and structure learning in nested markov models. 2012. URL <http://arxiv.org/abs/1207.5058>. Preprint.

- Shpitser, I., Evans, R. J., Richardson, T. S., and Robins, J. M. Introduction to nested markov models. *Behaviormetrika*, 41(1):3–39, 2014.
- Silva, R. and Ghahramani, Z. Bayesian inference for gaussian mixed graph models. In *Proceedings of the Twenty-Second Annual Conference on Uncertainty in Artificial Intelligence (UAI-06)*, pages 453–460, 2006.
- Spirtes, P., Glymour, C., and Scheines, R. *Causation, Prediction, and Search*. Springer Verlag, 1993.
- Spirtes, P., Richardson, T., Meek, C., Scheines, R., and Glymour, C. Using path diagrams as a structural equation modelling tool. *Sociological Methods & Research*, 27(2):182–225, 1998.
- Verma, T. S. and Pearl, J. Equivalence and synthesis of causal models. In *Proceedings of the sixth annual Conference on Uncertainty in Artificial Intelligence (UAI-90)*, pages 220–227, 1991.
- Williams, L. Equivalent models: Concepts, problems, and alternatives. In *The Handbook of Structural Equation Modeling*, pages 247–260, 2012.
- Wright, S. The method of path coefficients. *The Annals of Mathematical Statistics*, 5(2):161–215, 1934.
- Wright, S. Path coefficients and path regressions: Alternative or complementary concepts? *Biometrics*, 16(2):189–202, 1960.